



HAL
open science

On robust LPV-based observation of fuel slosh dynamics for attitude control design

Jean-Marc Biannic, Anthony Bourdelle, H el ene Evain, Sabine Moreno,
Laurent Burlion

► To cite this version:

Jean-Marc Biannic, Anthony Bourdelle, H el ene Evain, Sabine Moreno, Laurent Burlion. On robust LPV-based observation of fuel slosh dynamics for attitude control design. IFAC LPVS 2019, Nov 2019, Eindhoven, Netherlands. hal-02870310

HAL Id: hal-02870310

<https://hal.science/hal-02870310>

Submitted on 16 Jun 2020

HAL is a multi-disciplinary open access archive for the deposit and dissemination of scientific research documents, whether they are published or not. The documents may come from teaching and research institutions in France or abroad, or from public or private research centers.

L'archive ouverte pluridisciplinaire **HAL**, est destin ee au d ep ot et  a la diffusion de documents scientifiques de niveau recherche, publi es ou non,  emanant des  tablissements d'enseignement et de recherche fran ais ou  trangers, des laboratoires publics ou priv es.

On robust LPV-based observation of fuel slosh dynamics for attitude control design

Jean-Marc Biannic* Anthony Bourdelle* H el ene Evain***
Sabine Moreno*** Laurent Burlion**

* ONERA-Toulouse (e-mail: biannic@onera.fr).
University of Toulouse, France.

** Rutgers University New Brunswick, NJ. USA.
*** CNES, Toulouse, France

Abstract: Most attitude control scenarios are highly affected by fuel slosh dynamics that must be carefully taken into account to preserve pointing accuracy. Since such dynamics are not easily predictable, standard strategies consist of bounding the performances of the control system to avoid interactions between the rigid dynamics of the spacecraft and the oscillating liquid motion inside the fuel tank. Thanks to a recently developed control-oriented CFD-based fuel slosh model, an alternative approach is evaluated in this paper. It is based on a reformulation of the slosh effects in the Linear-Parameter-Varying (LPV) framework from which a robust LPV observer is easily derived. The latter is then classically used in a disturbance compensation scheme. The proposed strategy is illustrated on a simple but realistic single axis attitude control scenario for a small satellite using reaction wheels.

Keywords: Slosh Dynamics, LPV Observers, Disturbance Compensation, Attitude Control.

1. INTRODUCTION

Most attitude control scenarios are highly affected by fuel slosh. This is especially true during aggressive maneuvers when fuel tanks are half empty. Unlike flexible dynamics induced by solar panels, the disturbance torque generated by the slosh effects has a relatively lower frequency action. At the price of lower performances, common strategies consist of avoiding interactions between the rigid dynamics of the spacecraft and those induced by the sloshing modes. The main advantage of such solutions, based on notch filters (see Preumont (1997) for example) is that they do not require any accurate sloshing torque model which is generally difficult to obtain. From the early work of Berry and Tegart (1975), the constant need for improved attitude control systems has led, until quite recently, to the development of more realistic control-oriented slosh models (see Bourdelle et al. (2019) and references therein for details). From a control design perspective, a common way to address sloshing is based on the equivalent mechanical model (see Mazzini (2015); Dodge et al. (2000); Vreeburg and Chato (2000); Sopasakis et al. (2015)). In such models, the mechanical parameters (mass, spring stiffness and pendulum length) are tuned to reproduce as well as possible, the liquid behavior. In Enright and Wong (1994) for example, Computational Fluid Dynamics (CFD) is used to evaluate sloshing frequencies and tune the aforementioned parameters. Based on such models, the control of spacecraft with multiple propellant sloshing modes has been addressed in Reyhanoglu and Rubio (2012) with both linear and Lyapunov-based nonlinear feedback controllers. Next,

advanced methods have been proposed in Hervas and Reyhanoglu (2012); Hervas et al. (2014) to take into account the consumption of propellant with time-varying parameters. In de Souza and de Souza (2014) pendulum model parameters are identified by a Kalman filter. Interestingly, the uncertainties in pendulum models can be addressed with robust control, as proposed in Yano and Terashima (2001) and further analyzed recently by Sopasakis et al. (2015) in the context of impulsively actuated spacecraft. These models, based on linearized fluid dynamics do generally not depend on angular speed or acceleration of the spacecraft, which however induce significant forces acting on the fluid. This is why, inspired by equivalent mechanical models, a generalization to nonlinear parameter-varying sloshing models along with a CFD-based parameter identification procedure was proposed in Bourdelle et al. (2019) to provide more realistic, control-oriented models. The observer-based attitude control design approach presented in this paper is supported by this model which is first rewritten in a Linear Parameter Varying (LPV) format. This class of systems has been extensively studied in the past twenty years and is well suited to many control design strategies among which observer-based techniques play a keyrole. See for example Hoffmann and Werner (2015) for a recent applications-oriented survey on LPV control techniques and Iulia-Bara et al. (2001) for further details on LPV-based observer design.

The remainder of the paper is organized as follows. In section 2, the attitude control problem is presented and the uncertain slosh LPV model is described. The need for slosh compensation is clearly emphasized in this section. Next, section 3 is devoted to the presentation of LPV-

* This work was supported by CNES

based observer design strategy through the resolution of fairly standard Linear Matrix Inequalities (LMIs). Next, the application of the proposed algorithm is detailed in section 4 and illustrated by various parameter-varying simulations. Concluding comments and future directions are finally given in section 5.

2. LPV MODEL DESCRIPTION

2.1 A brief presentation of the attitude control system

Based on data provided in Pittet and Arzelier (2006), the main objective of this paper is to evaluate the potential of LPV observer-based attitude control systems for a micro-satellite subject to slosh disturbances. Since coupling effects between the three axes of the satellite remain small, compared to the disturbance torques, we will focus on a single axis control problem. The open-loop dynamics then simply read:

$$J\ddot{\theta} = \Gamma_r + \Gamma_d + \Gamma_s \quad (1)$$

where $J = 30 \text{ kg.m}^2$ and θ denote the inertia of the satellite and its attitude angle respectively. Three different torques apply to this system.

The first one, denoted Γ_r is the control torque realized by a reaction wheel whose dynamics are represented by a second-order linear transfer function:

$$R_W(s) = \Gamma_r(s) / \tilde{\Gamma}_c(s) = \frac{1.2s + 0.75}{s^2 + 2.4s + 0.75} \quad (2)$$

This transfer function is applied to a saturated commanded torque $\tilde{\Gamma}_c$ resulting from the controller output Γ_c as follows (with $\Gamma_{max} = 0.005 \text{ N.m}$):

$$\tilde{\Gamma}_c(t) = \begin{cases} \text{sat}_{\Gamma_{max}}(\Gamma_c(t)) & \text{if } |H_w(t)| \leq H_{max} \\ 0 & \text{if } |H_w(t)| > H_{max} \end{cases} \quad (3)$$

where the kinetic momentum of the wheel verifies:

$$\begin{cases} \dot{H}_w(t) = \text{sat}_{\Gamma_{max}}(\Gamma_c(t)) \\ H_{max} = 0.12 \text{ kg.m}^2.\text{s}^{-1} \end{cases} \quad (4)$$

As is clear from (3), the bound H_{max} should be strictly avoided. Beyond this limit indeed the wheel can no longer be accelerated and suddenly stops producing any torque.

The second torque, denoted Γ_d captures all disturbances resulting from the satellite environment. During "short" maneuvers, it can be considered as a constant term:

$$\dot{\Gamma}_d = 0 \quad (5)$$

whose magnitude $\Gamma_d(0)$ rarely exceeds 10^{-5} N.m .

The last one, Γ_s to be further described next and extensively discussed throughout the paper, results from the effects of the slosh dynamics.

As a first step, the attitude control system is designed without explicitly taking into account any disturbance torque. To this purpose, a standard proportional-derivative controller is initially tuned with the following structure, where J is assumed to be known (or estimated):

$$\Gamma_c = K_p(\theta_r - \theta_m) + K_d(\dot{\theta}_r - \dot{\theta}_m) + J\ddot{\theta}_r \quad (6)$$

A possibly fast varying, but continuous acceleration profile $\ddot{\theta}_r$ is initially defined according to the objectives to be met. Next, $\dot{\theta}_r$ and θ_r are simply obtained by integration. Note that only θ_m – provided by a star tracker – is available

for feedback so that $\dot{\theta}_m$ is estimated with the help of a standard pseudo-derivation first-order filter $s/(1 + \tau.s)$ whose time constant $\tau = 0.5$ is tuned to reject sensor noises affecting θ_m with a reasonable delay. The proportional and derivative gains $K_p = 0.25$ and $K_d = 3.75$ are calculated by an output feedback partial pole placement technique so as to assign a well-damped second-order mode with $\omega_n = 0.1$ to enforce a settling time of less than 60 s. The results are presented in Figure 1. It can be observed that, **without any disturbance torque**, the reference signal on the attitude is perfectly tracked. After 60 s the residual error verifies $|\theta_r - \theta| \leq 0.05 \text{ deg}$ and is then twice smaller than the maximum allowed error $\epsilon_{max} = 0.1 \text{ deg}$. On the other hand, a small discrepancy is visible on the acceleration signal which cannot perfectly track the reference because of the actuator which, however, does not saturate.

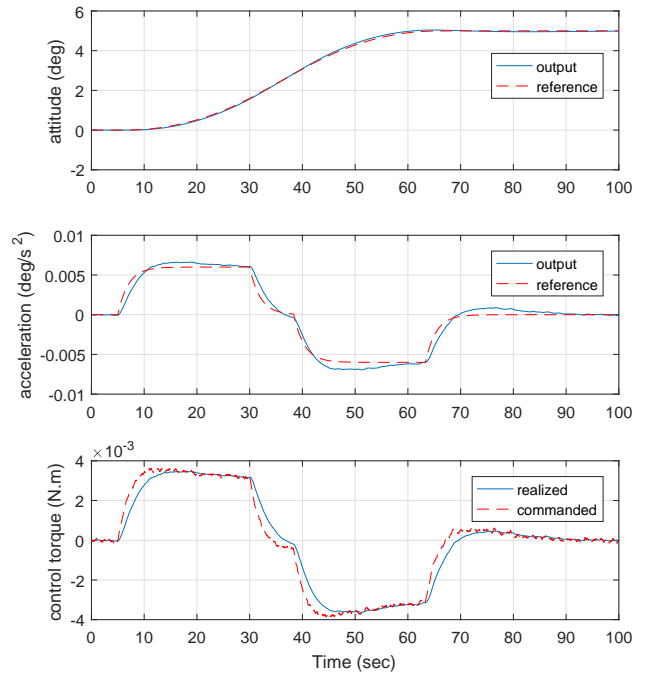


Fig. 1. Nominal simulations **without sloshing effects**

2.2 LPV modeling of the sloshing torque

Let us now introduce the sloshing effects, captured by the disturbance torque Γ_d for which a control-oriented model was recently proposed in Bourdelle et al. (2019). The model is essentially based on a time-varying nonlinear and poorly damped second-order system:

$$\begin{cases} \ddot{\eta} &= -a_S(t)\dot{\theta} - b_S(t)\ddot{\theta} - c_S(t)\eta - k_S(t)\dot{\eta} \\ \Gamma_S &= \eta \\ |\eta(0)| &\leq \bar{\eta}_0, |\dot{\eta}(0)| \leq \bar{v}_0 \end{cases} \quad (7)$$

where the varying coefficients a_S, b_S, c_S, k_S mainly depend on the angular velocity ($\dot{\theta}$) and acceleration ($\ddot{\theta}$). Extensive simulations have also revealed strong correlations between a_S and b_S on the one hand, and between c_S and k_S on the other, allowing those to be rewritten as follows:

$$\begin{cases} a_S(t) = a_0 + \alpha(t).a_1 \\ b_S(t) = b_0 + \alpha(t).b_1 \end{cases} \quad \begin{cases} c_S(t) = c_0 + \beta(t).c_1 \\ k_S(t) = k_0 + \beta(t).k_1 \end{cases} \quad (8)$$

where $\alpha(t) \in [-1, 1]$ and $\beta(t) \in [-1, 1]$ are normalized parameters that can be approximated by functions whose time dependence is now implicit:

$$\alpha(t) \approx \hat{\alpha}(\dot{\theta}, \ddot{\theta}), \quad \beta(t) \approx \hat{\beta}(\dot{\theta}, \ddot{\theta}) \quad (9)$$

The coefficients are summarized in Table 1.

a_0	a_1	b_0	b_1	c_0	c_1	k_0	k_1	$\bar{\eta}_0$	$\bar{\nu}_0$
5	7	20	-35	23	8	8	4	3	0.3

Table 1. Slosh parameters $\times 1000$

In order to justify the need for slosh compensation, preliminary simulations are performed in nominal conditions for which the coefficients in (8) are assumed to be constant with $\alpha(t) = \beta(t) = 0$. The initial conditions in (7) are chosen as $\eta(0) = -3.10^{-3}$ and $\dot{\eta}(0) = -3.10^{-4}$. In addition, the magnitude of the constant disturbance torque Γ_d introduced in (1) is also fixed to -3.10^{-4} which is rather high. The proportional-derivative control law is initially applied and produces the results displayed by the blue plots in Figure 2. As one could expect, the pointing performance is poor and it takes almost 200 s before the error verifies the required specification $|\theta_r - \theta| \leq 0.1 \text{ deg}$. This is not surprising since the sloshing torque (visualized in the last subplot of Figure 2) exhibits significant variations whose amplitude nearly reaches half of the maximum achievable control torque.

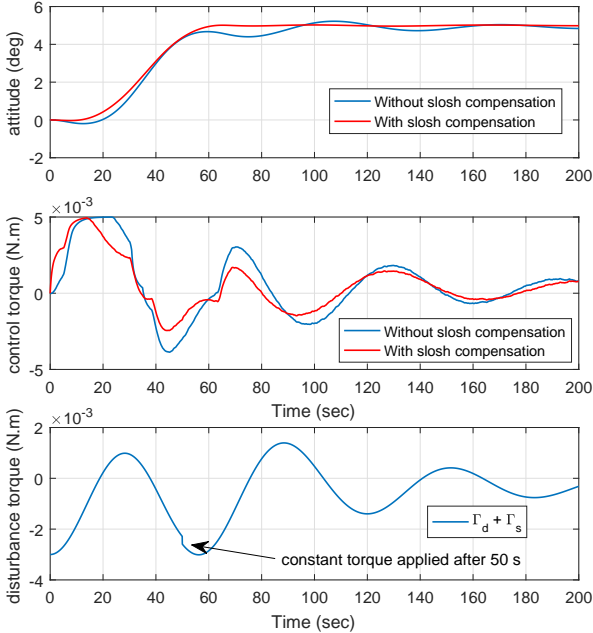


Fig. 2. Nominal simulations **with sloshing effects**

Assuming (which is not true in practice!) that the total disturbance torque is available for feedback, an "ideal" control law $\tilde{\Gamma}_c = \Gamma_c - \Gamma_d - \Gamma_s$ is applied that directly compensates the undesirable torques. The results, visualized in red, demonstrate the effectiveness of this unfortunately non realistic approach. The desired attitude angle is now

reached in less than 60 s. This also clearly illustrates the need for the design of a parameter-dependent and robust observer that permits to obtain an accurate estimation of the sloshing torque despite its time-varying properties and the uncertainties that affect the model. This is the main objective of the following section.

3. LPV OBSERVER DESIGN

3.1 Observer structure and problem statement

Combining equations (1), (2), (5), (7), (8) and (9) the open-loop model can be rewritten in the standard following compact form:

$$\begin{cases} \dot{x} = A(p(t))x + B_1(p(t))w + B_2(p(t))u \\ z = C_1(p(t))x + D_{11}(p(t))w = \Gamma_s + \Gamma_d \\ y = C_2x + D_{21}w = \theta_m \end{cases} \quad (10)$$

where the varying parameter $p(t) = [\hat{\alpha}(x(t)) \hat{\beta}(x(t))]'$ is assumed available for feedback and the perturbation term $B_1(p(t))w$ is introduced to capture the mismatch between the "true" parameters $\alpha(t)$ and $\beta(t)$ defined in (8) and their respective approximations. The input perturbation w is also used to introduce noise on the measured attitude angle $y = \theta_m$. As is clarified above, the objective is to obtain a reliable estimate of the total disturbance torque $z = \Gamma_s + \Gamma_d$. For this purpose, a straightforward parameter-dependent extension of the standard Luenberger state observer is used:

$$\begin{cases} \dot{\hat{x}} = A(p(t))\hat{x} + B_2(p(t))u + L(p(t))(y - C_2\hat{x}) \\ \hat{z} = C_1(p(t))\hat{x} \end{cases} \quad (11)$$

It is then readily checked that the errors $\epsilon_x = x - \hat{x}$ and $\epsilon_z = z - \hat{z}$ verify:

$$\begin{cases} \dot{\epsilon}_x = (A(p) - L(p)C_2)\epsilon_x + (B_1(p) + L(p)D_{21})w \\ \epsilon_z = C_1(p)\epsilon_x + D_{11}(p)w \end{cases} \quad (12)$$

where the time-dependence in $p(t)$ has been dropped out for compactness. With this choice, the observer design problem "reduces" to the optimization of a parameter-dependent gain $L(p)$ such that:

- the LPV system (12) remains stable for any admissible parametric trajectory,
- the error ϵ_z is reduced and kept as small as possible despite possibly adverse initial conditions and non negligible input perturbations.

By introducing a quadratic Lyapunov function $V(\epsilon_x) = \epsilon_x'X\epsilon_x$, the first objective is easily enforced, independently of the input w , as soon as a positive definite matrix X can be found such that:

$$\dot{V}(\epsilon_x) + 2\tau^{-1}V(\epsilon_x) < 0 \quad (13)$$

where the time-constant τ is tuned to control the convergence rate of the observation error. Moreover, if V , for positive scalars λ and μ , can be chosen such that:

$$\dot{V}(\epsilon_x) - \lambda w'w + \mu^{-1}z_\epsilon'z_\epsilon < 0 \quad (14)$$

then, by integration one obtains:

$$\int_0^\infty z_\epsilon'z_\epsilon dt < \lambda\mu \int_0^\infty w'w dt + \mu \epsilon_x(0)'X\epsilon_x(0) \quad (15)$$

According to the weights either applied on λ or μ in the optimization process, the designed observer gain can exhibit different robustness properties against adverse

initial conditions (small μ) or worst-case perturbations captured in w (for small $\lambda\mu$).

3.2 LMI-based characterization

Boyd et al. (1994) Combining inequalities (13) and (14) with state-space equations (12), it is easily verified that the Lyapunov function defined by $X > 0$ and the observer gain $L(p)$ defined through the auxiliary variable $Y(p)$ are characterized as the solutions of the parameter dependent matrix inequalities:

$$\begin{pmatrix} \Psi(p) + \Psi'(p) & XB_{1i}(p) + Y(p)D_{21} & C_{1i}(p)' \\ B_{1i}(p)'X + D_{21}'Y(p)' & -\lambda I_m & D_{1i}(p)' \\ C_{1i}(p) & D_{1i}(p) & -\mu I_p \end{pmatrix} < 0 \quad (16)$$

with

$$\Psi(p) = X(A(p) + \tau^{-1}I) - Y(p)C_2 \quad (17)$$

and

$$Y(p) = XL(p) \quad (18)$$

For practical reasons, it is often useful to bound the observer gains which is not directly feasible in the above inequality where a change of variable (18) has been introduced. However, assuming that $X > I^{-1}$, it is easily checked that:

$$\begin{pmatrix} \rho I & Y(p)' \\ Y(p) & X \end{pmatrix} > 0 \Rightarrow \begin{pmatrix} \rho I & Y(p)' \\ Y(p) & X^2 \end{pmatrix} > 0 \quad (19)$$

$$\Rightarrow L(p)'L(p) < \rho I$$

In our context, the parametric dependence in (12) is affine so that the infinite number of matrix inequalities that appear in (16) is equivalently transformed into a finite number corresponding to the N vertices:

$$p(t) \in \mathcal{C}_o\{p_1, p_2, \dots, p_N\} \quad (20)$$

In addition, it can also be reasonably assumed that the set of all admissible initial conditions $\epsilon_x(0)$ belongs to a polytope with q vertices, so that:

$$\epsilon_x(0) \in \mathcal{C}_o\{\xi_1, \xi_2, \dots, \xi_q\} \quad (21)$$

With the above assumptions in mind, and denoting for compactness any vertex of the form $Z(p_i)$ by the shortcut Z_i , the following LMI-based characterization can be proposed as a flexible optimization framework to compute the vertices of a bounded LPV observer gains $L(p) \in \mathcal{C}_o\{L_1, L_2, \dots, L_N\}$:

Algorithm 1. LPV observer design.

- (1) initialization
 - Fix positive scalars ρ and τ
 - Select positive scalar weightings r_λ , r_μ and r_ν
- (2) solve the following linear objective minimization problem under LMI constraints:
$$\min_{X, Y_1 \dots Y_N} r_\lambda \cdot \lambda + r_\mu \cdot \mu + r_\nu \cdot \nu \quad \forall i = 1 \dots N, \quad \forall j = 1 \dots q :$$

$$\begin{pmatrix} \Psi_i + \Psi_i' & XB_{1i} + Y_i D_{21} & C_{1i}' \\ B_{1i}'X + D_{21}'Y_i' & -\lambda I_m & D_{1i}' \\ C_{1i} & D_{1i} & -\mu I_p \end{pmatrix} < 0 \quad (22)$$

¹ This assumption is not restrictive. If the quadruple (X, Y, λ, μ) verifies the inequality (16), then this also the case of $(\eta X, \eta Y, \eta \lambda, \eta^{-1} \mu)$ for any positive real η .

$$\begin{pmatrix} \rho I & Y_i' \\ Y_i & X \end{pmatrix} > 0, \quad X > I \quad (23)$$

$$\xi_j' X \xi_j < \nu, \quad j = 1, \dots, q \quad (24)$$

(3) Compute $L_i = Y_i X^{-1}$.

Remark 1. Note, by a convexity argument, that the inequalities (24) imply that for all $\epsilon_x(0)$ in the polytope defined by (21), $V_0 = \epsilon_x(0)' X \epsilon_x(0) \leq \nu$, and then:

$$\int_0^\infty z_\epsilon' z_\epsilon dt < \lambda \mu \int_0^\infty w' w dt + \mu \nu \quad (25)$$

Remark 2. With the selection $(r_\lambda, r_\mu, r_\nu) = (1, 0, 0)$ and setting $\lambda = \mu$ in inequality (22), one obtains the standard solution that minimizes the \mathcal{L}_2 induced gain from w to z_ϵ .

Remark 3. Note that the above characterization remains convex in the "robust" case with $L_1 = L_2 = \dots = L_N$. Convexity is lost however when using a parameter-dependent Lyapunov function $X \rightarrow X(p)$. In that case, the LMI tests (22) at the vertices of the polytope are no longer sufficient but a denser grid including inner points must be considered. This generally leads to heavier calculations with a significant increase both in the number of decision variables and constraints. It also requires to check *a posteriori* that the solution remains valid on the whole parametric domain Biannic et al. (2011). This approach has not been considered in this application since satisfying solutions were found with fixed Lyapunov functions.

4. APPLICATION & SIMULATION RESULTS

4.1 Derivation of the polytopic design model

A polytopic representation of the parameter-varying system (10) is obtained with the help of a Simulink diagram (see Figure 3) which is evaluated at the 4 vertices of the parametric domain corresponding to $\alpha = \pm 1$ and $\beta = \pm 1$ (see equation (8)).

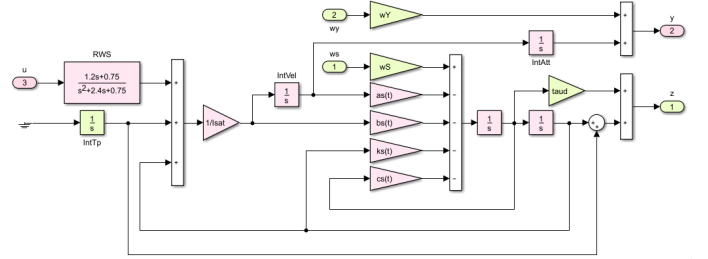


Fig. 3. A Simulink view of the design model

Remark 4. The output $z = \Gamma_s + \Gamma_d$ to be estimated by the LPV observer is slightly modified with an anticipating term $z \leftarrow z + \tau_d \dot{\Gamma}_s$. The parameter τ_d is tuned in such a way that the norm $\|\Gamma_d + \Gamma_s - z_{rw}\|$ is minimized where z_{rw} denotes the response of the reaction wheel system to the input z . With reference to equation (2), the parameter τ_d is obtained as:

$$\tau_d = \arg \min_{\tau} \|(1 + \tau s)R_W(s) - 1\|_\infty \approx 1 \quad (26)$$

Remark 5. In addition to the general description of section 3, note that the disturbance input signal w is split in two signals w_s (that affects the slosh model) and w_y (that affects the measurement). Weighting functions W_s and W_y are used to penalize the slosh model or the noise respectively.

4.2 Optimization process

The design algorithm 1 is now applied with $r_\lambda = r_\mu = 1$, $r_\nu = 0$ and fixing $\nu = 1$. The weightings W_s and W_y are respectively set to 0.01 and 0.1. As observed in Remark 3, the algorithm is easily adapted to the optimization of a fixed gain L (by fixing $Y_i = Y$) while preserving convexity. The two options have then been considered and the results are presented in Table 2.

	varying gain $L(p)$	fixed gain L
λ	0.85	0.97
μ	1.43	1.87
$\gamma = \sqrt{\lambda\mu}$	1.10	1.35

Table 2. LMI optimization results

As expected the varying gain $L(p)$ permits to further minimize λ and μ although the improvement is not that significant. It is important however to keep in mind, from equation (11), that the implemented observer remains parameter varying even though L is a constant matrix.

4.3 Implementation and simulation results

The above LPV disturbance torque observer is now combined with the proportional-derivative attitude control law (6) and tested for different noise profile on the attitude measurement and various initial conditions. Moreover, during simulations, parametric variations are arbitrarily applied in the interval $[-1, 1]$ to the normalized coefficients $\alpha(t)$ and $\beta(t)$ that affect the slosh model. Finally, a 30% time-varying multiplicative uncertainty is also introduced on both coefficients. As a result, the varying parameters used by the observer (denoted $\hat{\alpha}$ and $\hat{\beta}$) differ from the nominal ones. The implemented attitude control law then reads:

$$\begin{cases} \dot{\hat{x}} = A(\hat{\alpha}, \hat{\beta}) \hat{x} + B_2 u + L(\hat{\alpha}, \hat{\beta})(\theta_m - C_2 \hat{x}) \\ \Gamma_c = K_p(\theta_r - \theta_m) + K_d(\dot{\theta}_r - \dot{\hat{\theta}}_m) + \hat{J}\ddot{\theta}_r - C_1 \hat{x} \end{cases} \quad (27)$$

With the above controller, the simulation initially presented in Figure 2 is now replayed and visualized below (see Figure 4).

The upper subplot reveals a perfect tracking of the attitude angle which is stabilized to the desired value after 60 s. The residual error then remains below 0.05 deg. The second subplot shows that the control activity tends to be slightly lower when the compensation scheme is activated although in both cases (with and without compensation) the magnitude bounds are reached. The last subplot shows the evolution of the total disturbance torque (blue line) and its estimation (red line). The initial condition was fixed to $\Gamma_{S_0} = -3 \cdot 10^{-3}$. Next, a constant disturbance torque with magnitude $\Gamma_d = -3 \cdot 10^{-4}$ is applied after 50 s. It can be observed that the estimated torque matches well the real disturbance after 60 s.

Next, another simulation is performed with a different initial condition (see Figure 5). The initial torque is now reduced to $\Gamma_{S_0} = -5 \cdot 10^{-4}$ and, quite unexpectedly, it

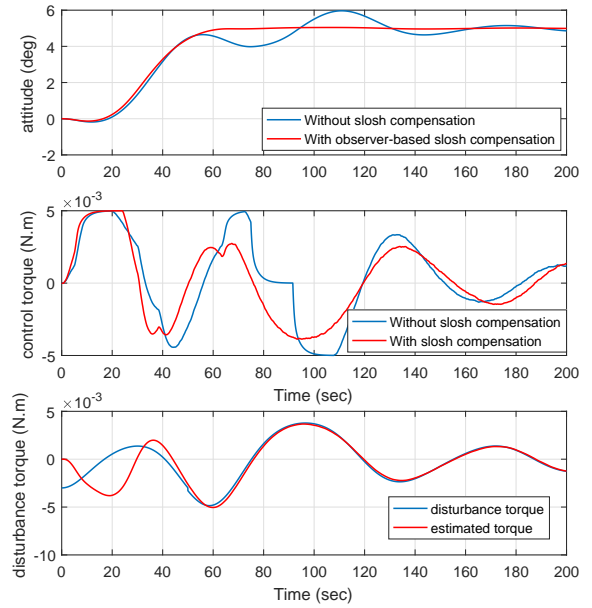


Fig. 4. Parameter-varying simulations **with sloshing effects** - Initial condition on sloshing $\Gamma_{S_0} = -3 \cdot 10^{-3}$

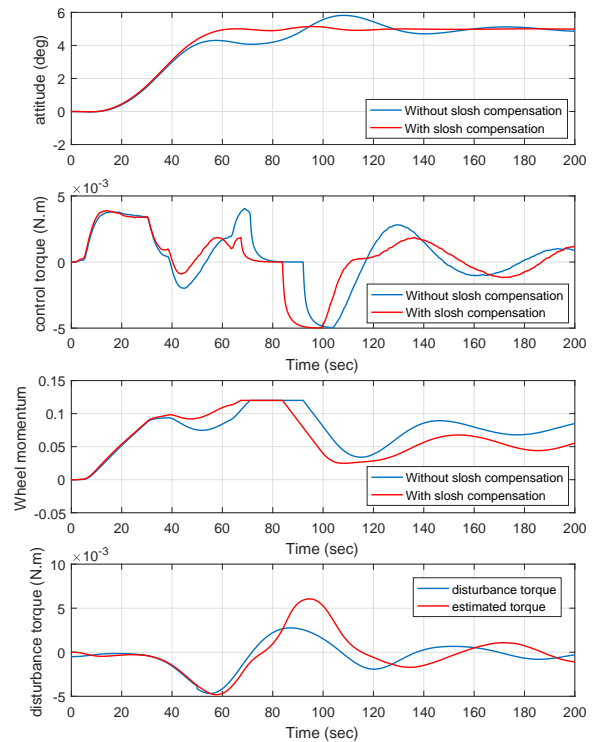


Fig. 5. Parameter-varying simulations **with sloshing effects** - Initial condition on sloshing $\Gamma_{S_0} = -5 \cdot 10^{-4}$

now takes more than 100 s before the tracking objective $|\theta_r - \theta| < 0.1$ is reached.

This "anomaly" is easily explained by the third subplot of Figure 5 which shows the kinetic momentum of the

reaction wheel. As mentioned in section 2, the latter is limited to ± 0.12 . Obviously, the upper bound is reached slightly after 60 s so that the produced torque is canceled out. This nonlinear behavior of the reaction wheel system is not implemented in the LPV observer whose output no longer matches the true disturbance torque.

5. CONCLUSION

Based on a recently developed control-oriented CFD-based fuel slosh model, an LPV reformulation has been proposed in this paper which then permitted to design an LPV-based observer of the total disturbance torque. Following a standard scheme, the latter has then been used to design an improved attitude control system. In the absence of saturation in the reaction wheel system, the proposed observer-based controller has proven to be very efficient despite uncertainties and adverse initial conditions. Moreover, it appeared that a "reasonable" magnitude saturation does not significantly impact the result. This is however not the case of the saturation that affects the kinetic momentum of the wheel which should be strictly avoided. Various strategies, based in particular on explicit reference governors techniques (see Nicotra et al. (2019)) will be proposed and compared in a near future to take such strong limitations into account.

REFERENCES

- Berry, R.L. and Tegart, J.R. (1975). Experimental study of transient liquid motion in orbiting spacecraft (nasa-cr-144003). Technical report.
- Biannic, J.M., Roos, C., and Pittet, C. (2011). Linear Parameter Analysis of Switched Controllers for Attitude Control Systems. *Journal of Guidance, Control and Dynamics*, 34(5), 1561–1567.
- Bourdelle, A., Burlion, L., Biannic, J.M., Evain, H., Moreno, S., Pittet, C., Dalmon, A., Tanguy, S., and Ahmed-Ali, T. (2019). Towards New Controller Design Oriented Models of Propellant Sloshing in Observation Spacecraft. In *Proceedings of the AIAA SciTech Forum*. San Diego, California.
- Boyd, S., El Ghaoui, L., Feron, E., and Balakrishnan, V. (1994). *Linear Matrix Inequalities in System and Control Theory*. SIAM studies in applied mathematics: 15.
- de Souza, L.C.G. and de Souza, A.G. (2014). Satellite attitude control system design considering the fuel slosh dynamics. *Shock and Vibration*, 2014.
- Dodge, F.T. et al. (2000). *The new "Dynamic Behavior of Liquids in Moving Containers"*. S.W. Research Inst. San Antonio, TX.
- Enright, P.J. and Wong, E.C.. (1994). Propellant slosh models for the cassini spacecraft. Technical report, Jet Propulsion Laboratory, Caltech.
- Hervas, J., , and Reyhanoglu, M. (2014). Observer-based nonlinear control of space vehicles with multi-mass fuel slosh dynamics. In *2014 IEEE 23rd International Symposium on Industrial Electronics (ISIE)*, 178–182.
- Hervas, J. and Reyhanoglu, M. (2012). Control of a spacecraft with time-varying propellant slosh parameters. In *Control, Automation and Systems (ICCAS), 2012 12th International Conference on*, 1621–1626. IEEE.
- Hoffmann, C. and Werner, H. (2015). A survey of linear parameter-varying control applications validated by experiments or high-fidelity simulations. *IEEE Transactions on Control Systems Technology*, 23(2), 416–433.
- Iulia-Bara, G., Daafouz, J., Kratz, F., and Ragot, J. (2001). Parameter-dependent state observer design for affine lpv systems. *International Journal of Control*, 74(16), 1601–1611.
- Mazzini, L. (2015). *Flexible Spacecraft Dynamics, Control and Guidance*. Springer.
- Nicotra, M., Liao-McPherson, M., Burlion, L., and Kolmanovskiy, I. (2019). Spacecraft attitude control with nonconvex constraints: An explicit reference governor approach. *arXiv preprint arXiv:1905.00387*.
- Pittet, C. and Arzelier, D. (2006). 'demeter: a benchmark for robust analysis and control of the attitude of flexible micro satellites'. In *Proceedings of the 5th IFAC Symposium on Robust Control Design (ROCOND'06)*. Toulouse, France.
- Preumont, A. (1997). *Vibration control of active structures*, volume 2. Springer.
- Reyhanoglu, M. and Rubio, H. (2012). Nonlinear dynamics and control of space vehicles with multiple fuel slosh modes. *Control Engineering Practice*, 20(2), 912–918.
- Sopasakis, P., Bernardini, D., Strauch, H., Bennani, S., and Bemporad, A. (2015). Sloshing-aware attitude control of impulsively actuated spacecraft. In *2015 European Control Conference (ECC)*, 1376–1381.
- Vreeburg, J. and Chato, D. (2000). Models for liquid impact onboard sloshsat flevo. In *Space 2000 Conference and Exposition*, 5152.
- Yano, K. and Terashima, K. (2001). Robust liquid container transfer control for complete sloshing suppression. *IEEE Transactions on Control Systems Technology*, 9(3), 483–493.